Supporting Information for

# An efficient $Cu^{+}$ doped Gd-based fluoroaluminosilicate scintillator glass for X-ray detector

Guanlin He, Lianjie Li, Junyu Chen, Yujia Gong, Hai Guo*

Department of Physics, Zhejiang Normal University, Jinhua, 321004, China

* **Corresponding author:** Hai Guo, E-mail: ghh@zjnu.cn

## A. Experimental

### Preparation of glass samples:

A series of $Cu^+$ doped glass scintillators was prepared by melt quenching method. Raw materials include $SiO_2$ (A.R., from Sinopharm Chemical Reagent Co., Ltd.), $Al_2O_3$ (A.R., from Sinopharm Chemical Reagent Co., Ltd.), $SrF_2$ (C.P., from Meryer Biochemical Technology Co., Ltd.), $GdF_3$ (99.99%, from A&C Rare Earth Materials Center), $Cu_2O$ (99%, from Meryer Biochemical Technology Co., Ltd.) and aluminum powder (A.R., from Shanghai Zhanyun Chemical Co., Ltd.). First, the ingredients were thoroughly ground in an agate mortar for about 30 minutes. Then, the mixed powder was put into $Al_2O_3$ crucible and melted in air atmosphere at 1550 °C for 1 hour. The molten liquid was poured onto a copper plate preheated to 300 °C and pressed with another copper plate to obtain glass sample. The glass samples were annealed at 500 °C for 4 hours, and finally the samples were cut and polished to thickness of 2 mm for subsequent characterization.

### Characterizations of structural, luminescent and scintillating properties:

The X-ray diffraction (XRD) patterns of $Cu^+$ doped fluoroaluminosilicate glass were obtained by Rigaku MiniFlex/600 X-ray diffractometer (Tokyo, Japan). The Fourier transform infrared spectroscopy (FTIR) spectra of G-host and GCu3Al5.5 mixed with KBr powder at 1:10 ratio were obtained by using NEXUS 670 spectrophotometer (Massachusetts, USA). Transmittance spectra of 200-800 nm were measured by Hitachi U-3900 Ultraviolet-visible (UV-Vis) photometer (Tokyo, Japan). The photoluminescence excitation (PLE) spectra, photoluminescence (PL) spectra, internal quantum efficiency (IQE), external quantum efficiency (EQE), absorption efficiency (Abs) and fluorescence attenuation curves were obtained by Edinburgh FS5 fluorescence spectrometer (Livingston, UK) using xenon lamp as pump source. The refractive index ($n$) at 589 nm was measured by GI-RDB digital refractometer (Nanjing, China). The density ($\rho$) was measured according to Archimedes' principle by using deionized water as an immersion liquid. XEL spectra were acquired using the Zolix OmniFluo960 XEL spectrometer (Beijing, China) with X-ray tubes, and all samples

were compared with commercial $Bi_4Ge_3O_{12}$ (BGO) scintillator (2 mm). The BGO crystal was purchased from Shanghai Institute of Ceramics, Chinese Academy of Sciences, which is one of best quality suppliers of BGO crystal. The specific parameters were listed in following Table S1. X-ray images were taken with a Canon EOS 600D camera, and the GCu3Al5.5 glass was polished to 0.5 mm thickness for X-ray imaging. The XPS spectra were obtained by Thermo Scientific K-Alpha (Waltham, U.S.).

**Table S1** Parameters of BGO crystal from Shanghai Institute of Ceramics, Chinese Academy of Sciences.

| Parameter | Value |
|---|---|
| Density ($g/cm^3$) | 7.13 |
| Radiation length (cm) | 1.12 |
| Decay constant (ns) | 300 |
| Emission peak (nm) | 480 |
| Light output (ph/MeV) | 8000-9000 |
| Melting point (℃) | 1050 |
| Hardness (Mho) | 5 |
| Refractive Index | 2.15 |
| Hygroscopicity | none |
| Cleavage | none |

**B. The energy gap ($E_g$) between conduction band and valence band of the G-host**

The Relationship between $\alpha^2$ and $h\upsilon$ of G-host sample is displayed in Fig. S1. $E_g$ of G-host is calculated according to the following formula, [1]

$$\alpha = B(h\nu - E_g)^{\frac{1}{2}} \quad \text{(S1)}$$

where $\alpha$ stands for absorption coefficient, $B$ represents constant, $E_g$ is bandgap and $h\upsilon$ is photon energy, respectively.

The $\alpha$ is derived by converting transmittance data through $T = I/I_0$ and $I = I_0 e^{-\alpha d}$, where $T$, $I$, $I_0$ and $d$ stand for transmittance, transmitted intensity, incident intensity and thickness of glass. $E_g$ value of G-host is calculated to be 3.95 eV.

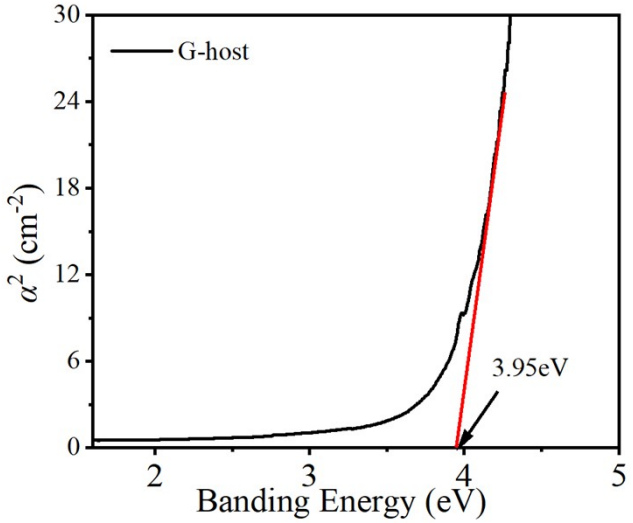


Fig. S1 Relationship between $\alpha^2$ and $h\upsilon$ of G-host sample with thickness of 2 mm.

**C. XPS spectra of GCu3Al5 and GCu3Al5.5 samples**

To further demonstrate the reduction process occurred in Al-doped samples, Fig. S2(a) and Fig. S2(b) show the high-resolution XPS spectra of Cu 2p of GCu3Al5 and GCu3Al5.5 samples, respectively. Four sharp peaks can be observed. The peaks at 932.6, 952.1, 933.6 and 953.8 eV are corresponded to $^2P_{3/2}$ orbit of $Cu^+$, $^2P_{1/2}$ orbit of $Cu^+$, $^2P_{3/2}$ orbit of $Cu^{2+}$ and $^2P_{1/2}$ orbit of $Cu^{2+}$, respectively.[2-5] When the content of Al increases, the integral area of $Cu^+$ increases significantly and that of $Cu^{2+}$ decreases rapidly. Therefore, the reduction process from $Cu^{2+}$ to $Cu^+$ has been clearly proved.

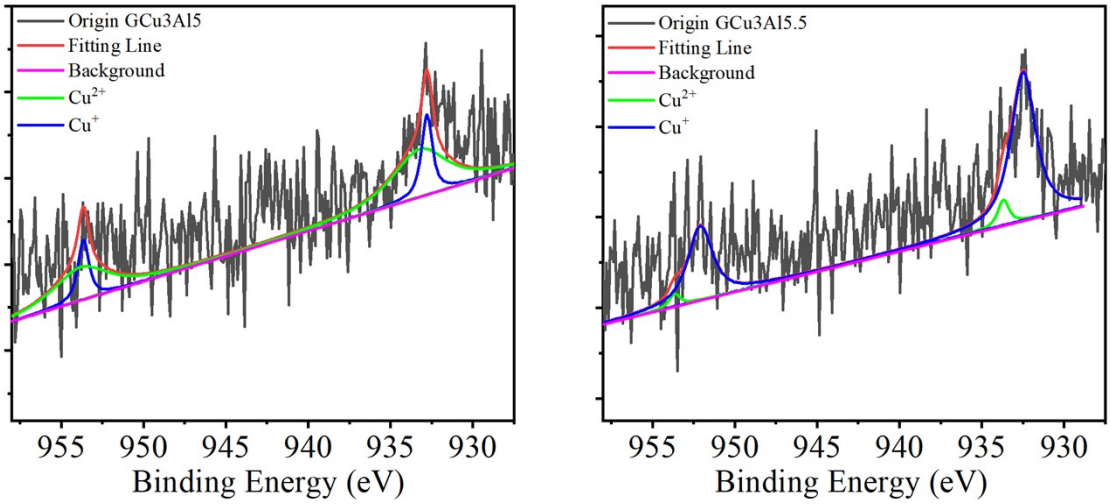


Fig. S2 High-resolution XPS spectra of Cu 2p of (a) GCu3Al5 and (b) GCu3Al5.5 samples.

**D. IQE, EQE and Abs of GCu3Al5.5 sample**

The IQE, EQE and Abs were tested under 291 nm and 273 nm excitation, as shown in Fig. S3(a) and S3(b), respectively. The IQE, EQE, and Abs can be calculated using the following equations,[6, 7]

$$\mathrm{IQE} = \frac{\int L_{\mathrm{sample}}}{\int E_{\mathrm{reference}} - \int E_{\mathrm{sample}}} \tag{S2}$$

$$\mathrm{EQE} = \frac{\int L_{\mathrm{sample}}}{\int E_{\mathrm{reference}}} \tag{S3}$$

$$\mathrm{Abs} = \frac{\mathrm{EQE}}{\mathrm{IQE}} \tag{S4}$$

where $L_{\mathrm{sample}}$ is the PL spectra of sample; $E_{\mathrm{reference}}$ and $E_{\mathrm{sample}}$ stand for the spectra of excitation light with $BaSO_4$ (as a reference) and sample, respectively; and the spectra were collected using an integrating sphere.

The IQE value of GCu3Al5.5 is 63.0% excited by 291 nm and 76.2% excited by 273 nm. The EQE value of GCu3Al5.5 is 55.3% excited by 291 nm and 66.7% excited by 273 nm. The Abs value of GCu3Al5.5 is 87.7% excited by 291 nm and 87.5% excited by 273 nm. The GCu3Al5.5 sample has high IQE, EQE and Abs, which symbolize that it might be a candidate for scintillator materials.

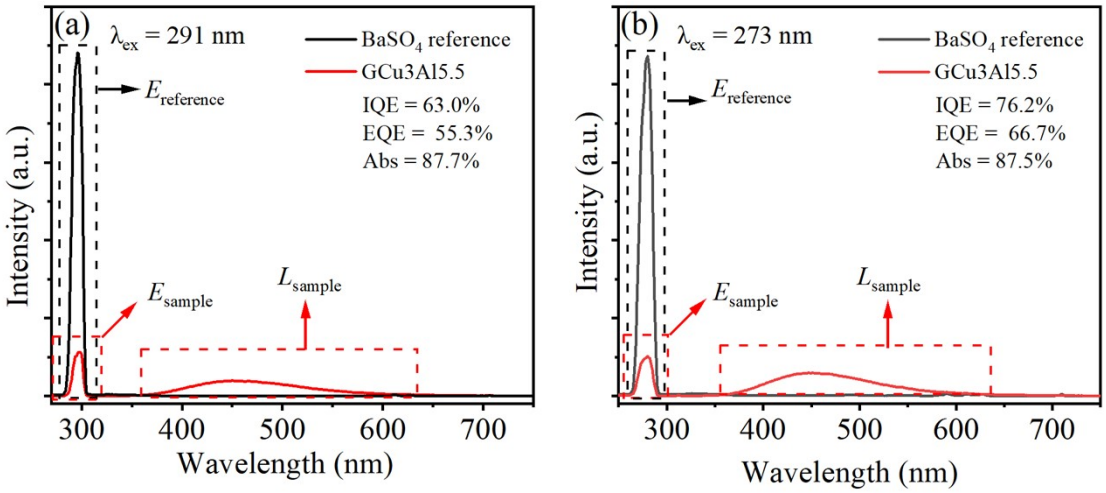


Fig. S3 (a) PL spectra ($\lambda_{ex}$ = 291 nm) and (b) PL spectra ($\lambda_{ex}$ = 273 nm) for measurement of IQE, EQE and Abs value by using an integrating sphere for GCu3Al5.5 sample.

**E. Effect of $GdF_3$ concentration on XEL intensity**

The effect of $GdF_3$ concentration on XEL intensity was investigated. The nominal compositions of samples are exhibited in Table S2 and their corresponding XEL spectra are shown in Fig. S4. With the increase of $Gd^{3+}$ concentration, the XEL intensity of glass samples first increase and then decrease. The optimal $GdF_3$ content is 7 mol%. Therefore, in this work, content of $GdF_3$ is fixed at 7 mol%.

**Table S2** The nominal concentrations of $SiO_2$, $Al_2O_3$, $SrF_2$, $GdF_3$, $Cu_2O$ and Al in each glass sample (in mol ratio).

| Sample | $SiO_2$ | $Al_2O_3$ | $SrF_2$ | $GdF_3$ | $Cu_2O$ | Al |
|---|---|---|---|---|---|---|
| GCu3Al5.5-Gd5 | 70 | 7 | 16 | 5 | 0.15 | 0.55 |
| GCu5Al5.5-Gd7 | 70 | 7 | 16 | 7 | 0.15 | 0.55 |
| GCu3Al5.5-Gd9 | 70 | 7 | 16 | 9 | 0.15 | 0.55 |

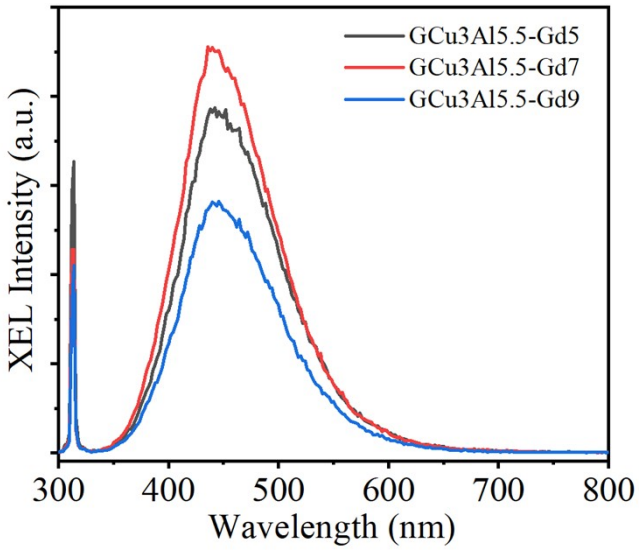


Fig. S4 XEL spectra of GCu3Al5.5-GdZ (Z = 5, 7, 9) samples.

**F. Refractive index ($n$), density ($\rho$) and effective atomic number ($Z_{eff}$) of GCuXAlY samples**

Refractive index ($n$), density ($\rho$) and effective atomic number ($Z_{eff}$) are fundamental and important parameters for glass scintillation. $Z_{eff}$ values are estimated by using the following formula,[8]

$$Z_{eff} = \sqrt[2.94]{f_1(Z_1)^{2.94} + f_2(Z_2)^{2.94} + \ldots + f_i(Z_i)^{2.94}} \quad \text{(S5)}$$

where $f_i$ is fraction of total number of electrons associated with each element, and $Z_i$ is atomic number of each element. These parameters of GCuXAlY samples are listed in Table S3.

**Table S3** The refractive index ($n$) at 589 nm, density ($\rho$) and effective atomic number ($Z_{eff}$) of GCuXAlY samples.

| Sample | $n$ | $\rho$ (g/cm$^3$) | $Z_{eff}$ |
|---|---|---|---|
| GCu1Al5.5 | 1.497 | 3.30 | 20.87 |
| GCu2Al5.5 | 1.522 | 3.31 | 20.87 |
| GCu3Al5.5 | 1.577 | 3.44 | 20.87 |
| GCu4Al5.5 | 1.550 | 3.51 | 20.87 |
| GCu5Al5.5 | 1.520 | 3.62 | 20.88 |
| GCu6Al5.5 | 1.516 | 3.64 | 20.88 |

**G. Details of irradiation properties of GCu3Al5.5**

The XEL spectra of GCu3Al5.5 are recorded every five minutes during 0-120 min. Fig. S5(a) shows these spectra. The XEL intensity of GCu3Al5.5 increases continuously in the first 40 minutes, then remains stable. And the final XEL intensity of GCu3Al5.5 is about 150% of its initial XEL intensity. Fig. S5(b) exhibits the transmittance spectra of GCu3Al5.5 sample before and after irradiation. After 120 min of irradiation, GCu3Al5.5 sample still maintain a high transmittance, indicating that GCu3Al5.5 sample has excellent radiation resistance capacity.

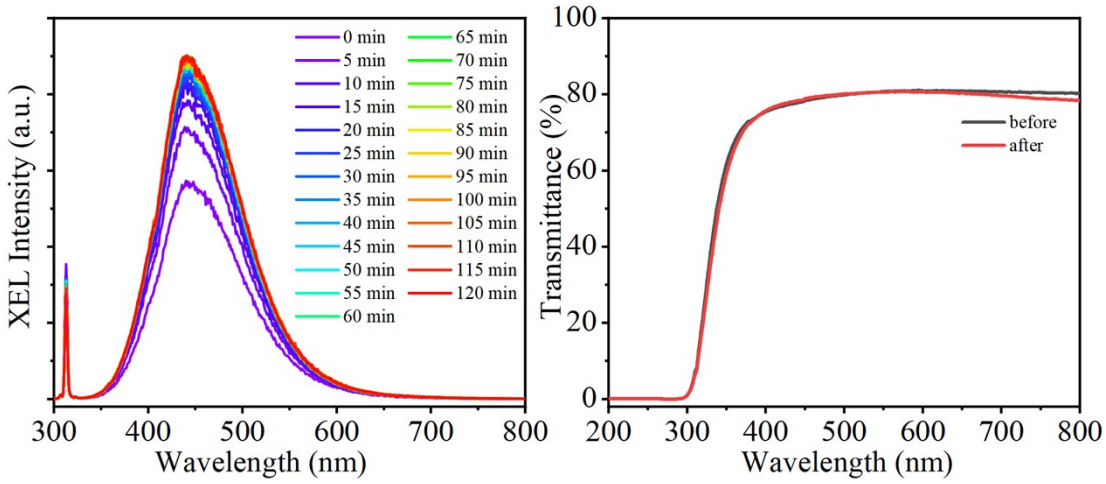


Fig. S5(a) XEL spectra of GCu3Al5.5 sample under continuous X-ray irradiation for 0- 120 min. (b) Transmittance spectra of GCu3Al5.5 sample before and after irradiation.

**H. Schematic diagram of equipment for X-ray imaging**

To assess the X-ray imaging performance of GCu3Al5.5, X-ray images of a chip, a capsule containing, a nail a capsule containing a spring and standard X-ray resolution test pattern plate were taken by home-made equipment for X-ray imaging, as shown in Fig. S6.

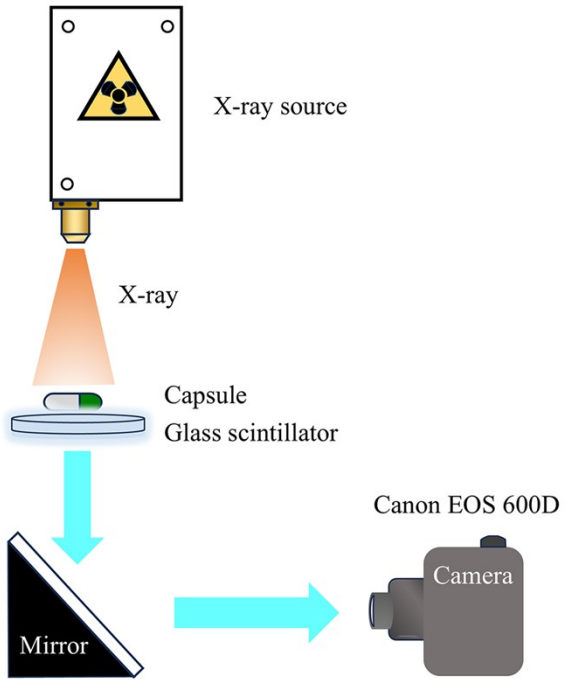


Fig. S6 Schematic diagram of the home-made equipment for X-ray imaging.

**Reference**


1. S. Y. Z. Chen, L. J. Li, J. Y. Chen, S. u. Xu, W. J. Huang, Z. X. Wen, T. M. Jiang and H. Guo, *J. Mater. Chem. C*, 2023, **11**, 2389-2396.
2. T. Ghodselahi, M. A. Vesaghi, A. Shafiekhani, A. Baghizadeh and M. Lameii, *Appl. Surf. Sci.*, 2008, **255**, 2730-2734.
3. J. A. Torres-Ochoa, D. Cabrera-German, O. Cortazar-Martinez, M. Bravo-Sanchez, G. Gomez-Sosa and A. Herrera-Gomez, *Appl. Surf. Sci.*, 2023, **622**, 156960.
4. S. Natesakhawat, J. W. Lekse, J. P. Baltrus, P. R. Ohodnicki, Jr., B. H. Howard, X. Deng and C. Matranga, *Acs Catal.*, 2012, **2**, 1667-1676.
5. D. V. Sivkov, O. V. Petrova, S. V. Nekipelov, A. S. Vinogradov, R. N. Skandakov, S. I. Isaenko, A. M. Ob'edkov, B. S. Kaverin, I. V. Vilkov, R. I. Korolev and V. N. Sivkov, *Nanomaterials*, 2021, **11**, 2993.
6. S. Y. Z. Chen, W. N. Zhang, L. M. Teng, J. Chen, X. Y. Sun, H. Guo and X. S. Qiao, *J. Eur. Ceram. Soc.*, 2021, **41**, 6722-6728.
7. S. Y. Z. Chen, Y. J. Gong, W. J. Huang, Z. X. Wen, L. J. Li, G. A. Ashraf, L. Lei, J. K. Cao and H. Guo, *J. Mater. Chem. C*, 2022, **10**, 10382-10388.
8. M. P. Singh, B. S. Sandhu and B. Singh, *Nucl. Instrum. Meth. A.*, 2007, **580**, 50-53.